

# Accurate event assignment from the decay-correlated mass measurement of the superheavy nuclide $^{257}\text{Db}$

Toshitaka Niwase<sup>a,\*</sup>, Peter Schury<sup>a</sup>, Michiharu Wada<sup>a</sup> and SHE-Mass collaborators

<sup>a</sup>KEK Wako Nuclear Science Center, Wako, Saitama 351-0198, Japan

Received November 3, 2022; Accepted January 12, 2023; Published online January 30, 2023

Decay-correlated mass spectroscopy using an  $\alpha$ -TOF detector is a new technique for doing decay spectroscopy of nuclides. Even for a small number of statistical events, with a yield of less than a few per day, the decay correlation can discriminate true events from background events, allowing accurate high-precision mass measurements to be made. In this paper, we discuss decay-correlated mass spectroscopy with a small number of statistics and the confidence level of the observed values based on their decay energies and decay times. We determined the mass of the superheavy element  $^{257}\text{Db}$  from 11 decay-correlated TOF detections with a precision of 1 ppm. This technique will be a major milestone in the path toward the comprehensive mass measurement of superheavy elements.

## 1. Introduction

Atomic mass is one of the most important static properties of nuclides. From Einstein's equation  $E=mc^2$ , scientists know that the binding energy of a nuclide corresponding to the requirement to stabilize the nucleus as a quantum many-body system can be observed as the nuclide's mass defect. As the binding energies reflect the nuclear structure and interaction of nucleons, high-precision mass measurements provide important information.

The multi-reflection time-of-flight mass spectrograph (MRTOF-MS) is one device for high-precision mass spectroscopy. Prior to 2015, the development and use of an MRTOF-MS for mass measurement of radioactive isotopes had only been reported by ISOLDE<sup>1</sup>, RIKEN<sup>2</sup> and GSI<sup>3</sup>. Since then, the construction and utilization of MRTOF-MS systems has spread to laboratories world-wide, including Argonne National Laboratory<sup>4</sup> and GANIL<sup>5</sup>. Several MRTOF-MSs are deployed at the RIKEN RIBF for comprehensive mass measurement covering all regions of the chart of the nuclides: fusion reaction products are measured in the SHE-Mass facility<sup>6</sup> combined with the gas-filled recoil ion separator GARIS-II<sup>7</sup>, multi-nucleon transfer products are measured in the system coupled with the KEK Isotope Separation System KISS<sup>8</sup>, and in-flight fission products are measured in the system<sup>9</sup> located behind the ZeroDegree (ZD) spectrometer<sup>10</sup> at BigRIPS.

Researchers of the SHE-Mass facility have recently succeeded in direct mass measurements of a superheavy nuclide  $^{257}\text{Db}$ <sup>11</sup>. The key technology enabling this measurement was a newly developed  $\alpha$ -TOF detector<sup>12</sup>. We embedded a silicon semiconductor detector (SSD) in a commercial time-of-flight (TOF) detector MagneTOF to produce the  $\alpha$ -TOF detector that enables correlated measurements of an ion's TOF and its subsequent radioactive decay signal. The  $\alpha$ -decay and spontaneous fission events are used as fingerprints to identify a nuclide – including its nuclear state – while significantly reducing the background. The development of decay-correlated mass measurements has opened a new frontier in nuclear spectroscopy research by enabling discrimination of isomers that could not be separated using the MRTOF-MS alone<sup>13</sup>. This  $\alpha$ -TOF detector allows for highly accurate identification of nuclides

with extremely small fusion reaction cross sections, such as superheavy elements, by distinguishing these rare events from background signals such as dark counts and contaminant ions.

In this paper, we detail event identification of the decay-correlated analysis of the mass measurement of  $^{257}\text{Db}$  which represents an investigation to assess the reliability of the  $\alpha$ -TOF detector used in combination with MRTOF-MS.

## 2. Experiment and results

Decay-correlated mass measurement of  $^{257}\text{Db}$  was performed at the SHE-Mass-II facility, jointly operated under the auspices of RIKEN Nishina Center and KEK Wako Nuclear Science Center, within the RIKEN RI Beam Factory. Details of the experimental setup are described elsewhere<sup>11</sup>. Atoms of the isotope  $^{257}\text{Db}$  were produced by the  $^{208}\text{Pb}(^{51}\text{V}, 2n)$  reaction. The evaporation residues were efficiently transported while the unreacted primary beam and other background products were suppressed by GARIS-II and were stopped and thermalized in a cryogenic helium gas cell at the focal plane. The thermalized ions were extracted from the gas cell using a traveling wave radio frequency (RF) carpet<sup>14</sup>, transported by a multiple RF ion trap and injected into the MRTOF-MS. The  $\alpha$ -TOF detector was used as the ion detector for the MRTOF-MS to obtain the ion arrival signal and subsequent  $\alpha$ -decay. The  $\alpha$ -TOF was energy calibrated by the  $\alpha$ -decays of  $^{185}\text{Hg}$  produced by the  $^{51}\text{V}+^{139}\text{La}$  reaction.

The TOF spectrum in the vicinity of  $^{257}\text{Db}^{3+}$  is shown in Figure 1(a). The upper part of the figure shows the time of arrival of the events, in chronological order of observation. The TOF values are plotted in terms of the TOF ratio  $\rho$  between  $^{257}\text{Db}^{3+}$  and the  $^{85}\text{Rb}^+$  reference ion, to normalize the values across different lap numbers. The correlation of the  $\alpha$ -decay signals detected within an arbitrary correlation time width from the TOF signals was taken. Details of the analysis are described in sect. 3.

In total, we observed 14 TOF decay-correlated event candidates during 105 hours of measurement. Figure 1(b) plots each decay-correlated event in terms of detected  $\alpha$ -decay energy and time between implantation and subsequent  $\alpha$ -decay;

\*Corresponding author. E-mail: tniwase@post.kek.jp

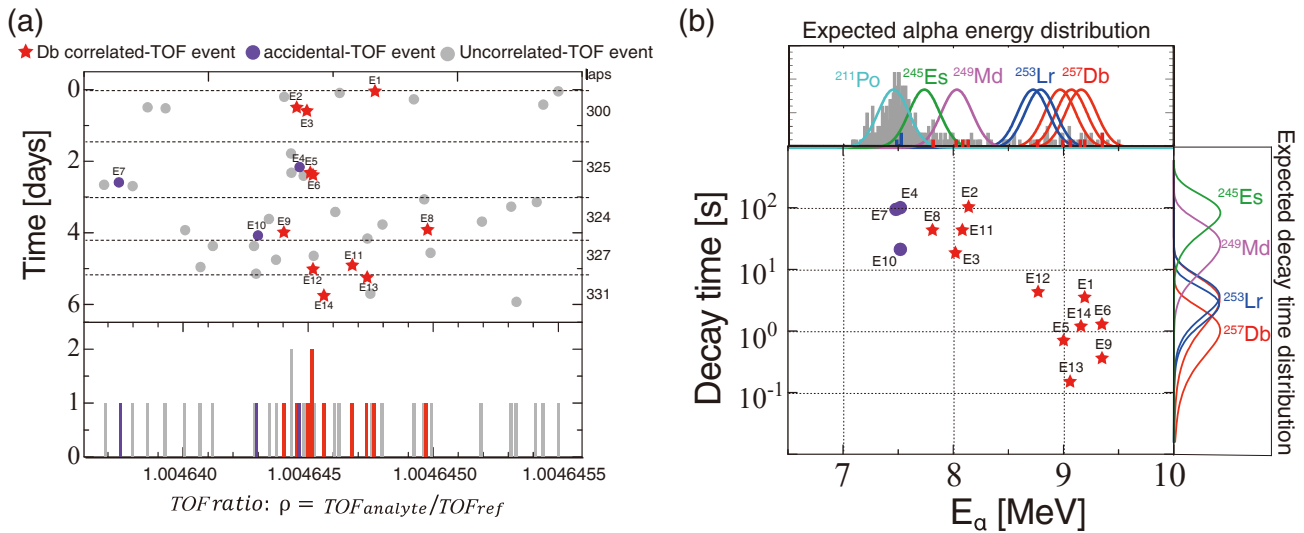


**Figure 1.** (a) The TOF spectrum and the time evolution of events near  $^{257}\text{Db}^{3+}$ . To normalize the flight time for different lap numbers, TOF ratio is plotted against the reference ion  $^{85}\text{Rb}^+$ . The absolute TOF is about 10 ms and the domain of the plot,  $\pm 10$  ppm, is about 200 ns. The red stars indicate the decay-correlated events of the  $^{257}\text{Db}$  decay chain and the purple circles indicate the accidentally-correlated events of the transfer products. (b) Two-dimensional distribution of TOF-correlated  $\alpha$ -decay events in a plot of decay energy vs. decay time. The probability distributions in terms of decay time are shown in the right panel, and the detector response function for  $\alpha$ -decay is shown in the top panel, superposed with the  $\alpha$ -singles spectrum with correlated event candidates denoted by colored marks.

events are named based on chronological order of observation. The right panel of Figure 1(b) shows the anticipated decay time probability distribution<sup>15</sup> for each nuclide; multiple curves are shown for  $^{257}\text{Db}$  and  $^{253}\text{Lr}$  to represent known isomers. The upper panel shows the expected energy distribution for each  $\alpha$ -decay which could be observed in the  $^{257}\text{Db}$  decay chain, with the  $\alpha$ -decay singles spectrum superimposed. The correlated events appear to fall into two clusters corresponding to  $^{257}\text{Db}$  or  $^{253}\text{Lr}$  (E1, E5, E6, E9, E12, E13, E14) and  $^{249}\text{Md}$  or  $^{245}\text{Es}$  (E2, E3, E4, E7, E8, E10, E11). Table 1 tabulates the decay energies and decay times of the 14 TOF decay-correlated events.

### 3. Discussion

The decay-correlation analysis begins with identifying candidate events by selecting  $\alpha$ -decay energy signals in the energy range consistent with  $\alpha$ -decays for the candidate nuclide. In the present experimental case, the energy gate range is 7.0 to 9.5 MeV, which corresponds to the energy range of the  $\alpha$ -decay chain from  $^{257}\text{Db}$  to  $^{245}\text{Es}$ . A TOF spectrum is then constructed from TOF events in the vicinity ( $\pm 100$  ns) of the expected location of  $^{257}\text{Db}$  occurring in a coincidence time ( $T_c$ ) prior to the  $\alpha$ -decay signal. The coincidence time is chosen according to the half-life of the analyte nuclides.

**3.1 Probability of a spurious correlation.** In this experiment, the coincidence time  $T_c$  for TOF- $\alpha$  decay correlations was chosen to be 120 s, which is sufficiently long enough to encompass decays of the granddaughter  $^{245}\text{Es}$ .

Using this  $T_c$ , the total number of  $\alpha$ -decay singles events in the analyte energy region ( $N_{\text{alpha}}$ ) and the total measurement time ( $T_{\text{total}}$ ), we estimated the random correlation probability  $P_{\text{random}}$ , defined by eq 1.

$$P_{\text{random}} = \frac{N_{\text{alpha}} \times T_c}{T_{\text{total}}} \times 100 [\%] \quad (1)$$

The random correlation probability in the energy region of  $^{211}\text{Po}$  was estimated to be 7.3%. This estimation was based on the 120 s coincidence time and 235 observed  $\alpha$ -decay counts in the  $^{211}\text{Po}$  energy region. There were 27 TOF singles events

observed in the TOF spectra in a 60 ns wide region centered on the expected TOF for  $^{257}\text{Db}^{3+}$  – the range corresponded to the full width at tenth maximum (FWTM) of the spectral peak based on the peak shape of the  $^{85}\text{Rb}^+$  reference ion. Therefore, we expected to observe  $\sim 2$  accidental correlations with  $^{211}\text{Po}$ . Similarly, the accidental correlation probabilities for islands in the  $^{257}\text{Db}$ - $^{253}\text{Lr}$  energy region and islands in the  $^{249}\text{Md}$ - $^{245}\text{Es}$  energy region were calculated to be 1.6% and 1.3%, respectively.

**3.2 Accuracy of each event.** Each of the experimentally obtained decay-correlated events was accurately determined by comparing the measured values to the known decay properties – decay energies and decay times – of the nuclide. The confidence level was evaluated as  $P(0,1) = 1 - g(z)$  using the area expressed as  $g(z) = \int_{-z}^z \frac{1}{\sqrt{2\pi}} \exp\left(-\frac{x^2}{2}\right) dx$  by integration of the probability density function of the standard normal distribution  $N(0,1)$ . For example, when the measured data point ( $z$ ) is  $1\sigma$  away from the central value, its confidence level  $P(0,1)$  is  $P = 1 - 0.683 = 0.317$ .

When there are  $n$  systems in parallel, each of which has a confidence level of  $X_i$ , the confidence level of the system as a whole,  $\Phi$ , can be written as  $\Phi = 1 - \prod_{i=1}^n (1 - X_i)$ . This evaluation is often used to evaluate the reliability of an entire system, such as a parallel circuit consisting of multiple systems<sup>16</sup>. The  $\alpha$ -decay energy and decay time of each event were compared to an arbitrary state of the nucleus of interest to evaluate the accuracy of the event. When the confidence level of the decay energy was set to  $P_{\text{ene}}$  and the confidence level of the decay time was set to  $P_{\text{dt}}$ , the accuracy of the acquired single event was evaluated as  $X_{\text{state}} = 1 - (1 - P_{\text{ene}})(1 - P_{\text{dt}})$  from the convolution by these parallel systems.

The nucleus to be compared is in one of several excited states, but in a system like Db, where the states are unknown and complex, it is difficult to distinguish individual states even with our mass resolving power and energy resolution. Thus, we assumed that each state existed in parallel, and the certainty of the acquired event  $\Phi_x$  could be expressed as a convolution of the accuracy of each state  $X_{\text{state}_x}$ .

$$\Phi_x = 1 - \prod_{\text{state}=1}^n (1 - X_{\text{state}_x}). \quad (2)$$

In the case of  $^{257}\text{Db}$ , three decay modes were intermingled, but this calculation allowed us to evaluate Db like the event itself, taking all states into account. Likewise, for  $^{253}\text{Lr}$  cases we could estimate the certainty from the convolution of the two states. Table 1 summarizes the certainty  $\Phi_x$  of each of the 14 decay-correlated events. The certainty  $\Phi_x$  was derived from the confidence level of the energy and decay time compared to the decay chain of  $^{257}\text{Db}$  and the multinucleon transfer product  $^{211}\text{Po}$ . Based on the reported decay properties, the states of  $^{257}\text{Db}$  corresponding to decay energies of 9.155 MeV, 9.066 MeV, and 8.965 MeV were tentatively assigned to  $^{257}\text{Db}(1)$ ,  $^{257}\text{Db}(2)$ , and  $^{257}\text{Db}(3)$ , respectively, and the states of  $^{253}\text{Lr}$  corresponding to decay energies of 8.719 MeV and 8.786 MeV were tentatively assigned to  $^{253}\text{Lr}(1)$  and  $^{253}\text{Lr}(2)$ , respectively. In the calculation, events with energy or decay time confidence less than  $2.5\sigma$ , i.e., less than  $P=0.01$ , were excluded from the calculation. The  $^{211}\text{Po}$  is due to accidental coincidence, so only the reliability of the energy was considered.

**3.3 Event assignments.** Based on the certainty  $\Phi_x$  shown in Table 1, the nuclide identification was performed for each of the decay-correlated events. For the energy uncertainties, the energy resolution of the  $\alpha$ -TOF detector,  $\sigma_E=140$  keV, was used.

**3.3.1 Events 1, 5, 6, 9, 13, 14.** For events 1, 5, 6, 9, 13, and 14 we measured  $\alpha$ -energies and decay times that were consistent with  $^{257}\text{Db}$ . Event 1 had the same degree of confidence for both  $^{257}\text{Db}(1)$  and  $^{257}\text{Db}(2)$  states. Events 5 and 14 had equal degrees of confidence for all states. Events 6, 9, and 13 were consistent only with  $^{257}\text{Db}(1)$ , tentatively assigned as the  $J^\pi=1/2^-$  isomeric state, from confidence calculations. The relative intensity of  $^{257}\text{Db}(1)$  is reported to be 19%<sup>17</sup>, and the expected number of events to reach this intensity is 1.14 out of 6 events. Given a Poisson distribution with an expected value of 1.14 events, the probability that the number of observed events is more than 3 is 11%. Based on the above reasoning, we determined that these 6 events were correlated with the decay of  $^{257}\text{Db}$ .

**3.3.2 Event 12.** Event 12 agreed with the decay properties of  $^{257}\text{Db}(3)$  and  $^{253}\text{Lr}(1)$  and  $^{253}\text{Lr}(2)$  with similar levels of confidence. The confidence level was slightly higher for  $^{253}\text{Lr}$  than for  $^{257}\text{Db}$ , thus event 12 was identified as  $^{253}\text{Lr}$ . Only one

Lr decay-correlation event was observed. Considering the branching ratio of  $\alpha$ -decay and the detection efficiency of the  $\alpha$ -TOF detector, the expected number of events was  $2.9 \pm 1.7$  counts. Our observed events were consistent with statistical fluctuations in the  $1.2\sigma$  range.

**3.3.3 Events 2, 3, 11.** The decay properties of events 2, 3, and 11 were in good agreement with those of  $^{249}\text{Md}$ , and the confidence levels of other nuclides were all below 0.01. Thus, we concluded that these three events were correlated with  $^{249}\text{Md}$  decay.

**3.3.4 Event 8.** The decay property of event 8 was consistent with the decay properties of  $^{245}\text{Es}$ , and it was far from the decay energy of  $^{211}\text{Po}$ , a multinucleon transfer reaction product. On the other hand, the detection probability for  $^{245}\text{Es}$  was only 1.4%, as described below, and the expected number to be observed from a total of 14 events was 0.3. When the expected value was 0.3, the probability of observing one event was 22%, which was not a small enough probability to reject. Also, if we assumed that this was the decay of  $^{249}\text{Md}$ , the decay time was consistent, but the decay energy was  $2.6\sigma$  away from the literature value<sup>17</sup>. Regardless of the nuclide identification, it was still an event correlated with the decay chain of  $^{257}\text{Db}$ , but we decided to trust the confidence level and to assume it was an event correlated with  $^{245}\text{Es}$  decay.

**3.3.5 Events 4, 7, 10.** The decay energies of events 4, 7, and 10 were in good agreement with the transfer product  $^{211}\text{Po}$ . The decay times for all events were close to those of  $^{245}\text{Es}$ , but the energies were more than  $2.5\sigma$  away. As discussed in sect. 3.1, the number of accidental coincidences in this energy region was estimated to be about 2, which was consistent with the observed number. Based on these evaluations, we determined that these three events were accidental coincidences with  $^{211}\text{Po}$  and we excluded them from the mass analysis.

Based on the above event assignments, we determined that 11 of the 14 events were attributable to  $^{257}\text{Db}$  and daughters, excluding the 3 events inferred to have been contributed by  $^{211}\text{Po}$ . The  $^{257}\text{Db}$  nuclide exhibits at least one long-lived isomeric state<sup>18</sup>. Neither the state order nor the isomeric excitation have been confirmed as yet. The NUBASE<sup>19</sup> recommends an isomeric excitation of 140 keV based on systematics. The present mass resolving power of the MRTOF-MS and  $\alpha$ -energy resolution of the  $\alpha$ -TOF detector cannot separate the

**TABLE 1: Summary of the certainty  $\Phi_x$  of each decay-correlated event compared to the nuclides in the  $^{257}\text{Db}$  chain**

	E $\alpha$ [MeV]	dt [s]	$\Phi$ ( $^{257}\text{Db}$ )	$\Phi$ ( $^{253}\text{Lr}$ )	$\Phi$ ( $^{249}\text{Md}$ )	$\Phi$ ( $^{245}\text{Es}$ )	$\Phi$ ( $^{211}\text{Po}$ )
E1	9.19	3.54	0.96	<0.01	<0.01	<0.01	<0.01
E2	8.14	105	<0.01	<0.01	0.56	<0.01	<0.01
E3	8.02	18.5	<0.01	<0.01	0.94	<0.01	<0.01
E4	7.52	100.2	<0.01	<0.01	<0.01	<0.01	0.38
E5	9.00	0.7	0.92	<0.01	<0.01	<0.01	<0.01
E6	9.35	1.3	0.92	<0.01	<0.01	<0.01	<0.01
E7	7.48	93.9	<0.01	<0.01	<0.01	<0.01	0.71
E8	7.81	44	<0.01	<0.01	<0.01	0.39	<0.01
E9	9.35	0.36	0.15	<0.01	<0.01	<0.01	<0.01
E10	7.52	21.1	<0.01	<0.01	<0.01	<0.01	0.38
E11	8.08	43.4	<0.01	<0.01	0.96	<0.01	<0.01
E12	8.77	4.3	0.92	0.99	<0.01	<0.01	<0.01
E13	9.06	0.15	0.82	<0.01	<0.01	<0.01	<0.01
E14	9.16	1.2	0.99	<0.01	<0.01	<0.01	<0.01

ground and isomeric states in  $^{257}\text{Db}$ . Therefore, we assumed that the measured events were split almost evenly between the two states, and we accounted for this by adding a systematic uncertainty of 70 keV/c<sup>2</sup>.

From these 11 highly accurate events, we determined the atomic mass of  $^{257}\text{Db}$  to be  $m(^{257}\text{Db})=257.10742(25)$  u and the mass excess to be  $\text{ME}(^{257}\text{Db})=100\,063(231)$  keV. This corresponded to a mass uncertainty of  $9.7 \times 10^{-7}$ , which was equivalent to a mass determination with a precision of 1 ppm.

#### 4. Conclusion

In this paper, we discussed in detail the event identification of the superheavy nuclide  $^{257}\text{Db}$  measured using a newly devised  $\alpha$ -decay-correlated mass measurement method. We strongly anticipate that such an identification method will accelerate further direct mass measurements of superheavy nuclides. Recently, we have also developed a  $\beta$ -TOF detector with two layers of SSDs forming a telescope designed to extend the technique to  $\beta$ -decaying nuclides. This technique will be expected to provide comprehensive mass measurements covering not only superheavy nuclides but also a wide range of nuclides in chart of the nuclides.

#### Acknowledgements

We express our gratitude to the RIKEN Nishina Center for Accelerator-based Science and the Center for Nuclear Science at University of Tokyo for their support of online measurements. This work was financially supported by the Japan Society for the Promotion of Science KAKENHI (Grant Nos. 17H06090 and No. 21J00670).

#### References

- [1] R.N. Wolf, F. Wienholtz, D. Atanasov, D. Beck, K. Blaum, C. Borgmann, F. Herfurth, M. Kowalska, S. Kreim, Y.A. Litvinov, D. Lunney, V. Manea, D. Neidherr, M. Rosenbusch, L. Schweikhard, J. Stanja, K. Zuber, *Int. J. Mass Spectrom.* **349–350** (2013) 123–133.
- [2] Y. Ito, P. Schury, M. Wada, S. Naimi, T. Sonoda, H. Mita, F. Arai, A. Takamine, K. Okada, A. Ozawa, H. Wollnik, *Phys. Rev. C* **88** (2013) 011306(R).
- [3] W. R. Plass, T. Dickel, C. Scheidenberger, *Int. J. Mass Spectrom.* **349–350** (2013) 134–144.
- [4] T. Y. Hirsh, N. Paul, M. Burkey, A. Aprahamian, F. Buchinger, S. Caldwell, J.A. Clark, A.F. Levand, L.L. Ying, S.T. Marley, G.E. Morgan, A. Nystrom, R. Orford, A.P. Galván, J. Rohrer, G. Savard, K.S. Sharma, K. Siegl, *Nucl. Instrum. Methods Phys. Res. B* **376** (C) (2016) 229–232.
- [5] P. Chauveau, P. Delahaye, G. de France, S. El Abir, J. Lory, Y. Merrer, M. Rosenbusch, L. Schweikhard, R.N. Wolf, *Nucl. Instrum. Methods Phys. Res. B* **376** (C) (2016) 211–215.
- [6] P. Schury, M. Wada, Y. Ito, D. Kaji, F. Arai, M. MacCormick, I. Murray, H. Haba, S. Jeong, S. Kimura, H. Koura, H. Miyatake, K. Morimoto, K. Morita, A. Ozawa, M. Rosenbusch, M. Reponen, P.A. Söderström, A. Takamine, T. Tanaka, H. Wollnik, *Phys. Rev. C* **95** (2017) 011305.
- [7] D. Kaji, K. Morimoto, N. Sato, A. Yoneda, K. Morita, *Nucl. Instrum. Methods Phys. Res. B* **317** (2013) 311–314.
- [8] Y. Hirayama, Y. X. Watanabe, N. Imai, H. Ishiyama, S. C. Jeong, H. Miyatake, M. Oyaizu, S. Kimura, M. Mukai, Y. H. Kim, T. Sonoda, M. Wada, M. Huyse, Yu. Kudryavtsev, P. Van Duppen, *Nucl. Instrum. Methods Phys. Res. B*, **353** (2015) 4–15.
- [9] M. Rosenbusch, M. Wada, S. Chen, A. Takamine, S. Iimura, D. Hou, W. Xian, S. Yan, P. Schury, Y. Hirayama, Y. Ito, H. Ishiyama, S. Kimura, T. Kojima, J. Lee, J. Liu, S. Michimasa, H. Miyatake, M. Mukai, J. Y. Moon, S. Nishimura, S. Naimi, T. Niwase, T. Sonoda, Y. X. Watanabe, H. Wollnik, arXiv:2110.11507.
- [10] T. Kubo, D. Kameda, H. Suzuki, N. Fukuda, H. Takeda, Y. Yanagisawa, M. Ohtake, K. Kusaka, K. Yoshida, N. Inabe, T. Ohnishi, A. Yoshida, K. Tanaka, Y. Mizoi, *Prog. Theo. Exp. Phys.* **2012** (2012) 03C003.
- [11] P. Schury, T. Niwase, M. Wada, P. Brionnet, S. Chen, T. Hashimoto, H. Haba, Y. Hirayama, D. S. Hou, S. Iimura, H. Ishiyama, S. Ishizawa, Y. Ito, D. Kaji, S. Kimura, H. Koura, J. J. Liu, H. Miyatake, J.-Y. Moon, K. Morimoto, K. Morita, D. Nagae, M. Rosenbusch, A. Takamine, Y. X. Watanabe, H. Wollnik, W. Xian, S. X. Yan, *Phys. Rev. C* **104**, (2021) L021304.
- [12] T. Niwase, M. Wada, P. Schury, H. Haba, S. Ishizawa, Y. Ito, D. Kaji, S. Kimura, H. Miyatake, K. Morimoto, K. Morita, M. Rosenbusch, H. Wollnik, T. Shanley, Y. Benari, *Nucl. Instrum. Methods Phys. Res. Sect. A* **953** (2020) 163198.
- [13] T. Niwase, M. Wada, P. Schury, P. Brionnet, S. D. Chen, T. Hashimoto, H. Haba, Y. Hirayama, D. S. Hou, S. Iimura, H. Ishiyama, S. Ishizawa, Y. Ito, D. Kaji, S. Kimura, J. Liu, H. Miyatake, J. Y. Moon, K. Morimoto, K. Morita, D. Nagae, M. Rosenbusch, A. Takamine, T. Tanaka, Y. X. Watanabe, H. Wollnik, W. Xian, S. X. Yan, *Phys. Rev. C* **104** (2021) 044617.
- [14] M. Wada, Y. Ishida, T. Nakamura, Y. Yamazaki, T. Kambara, H. Ohyama, Y. Kanai, T. M. Kojima, Y. Nakai, N. Ohshima, A. Yoshida, T. Kubo, Y. Matsuo, Y. Fukuyama, K. Okada, T. Sonoda, S. Ohtani, K. Noda, H. Kawakami, I. Katayama, *Nucl. Instrum. Methods Phys. Res. B*, **204** (2003) 570–581.
- [15] K. H. Schmidt, C. C. Sahn, K. Pielenz, H. G. Clerc, *Z. Phys. A* **316** (1) (1984) 19–26.
- [16] A. Kaufmann, D. Grouchko, R. Cruon, *Mathematical models for the study of the reliability of systems*, Volume 124, Academic Press (1977).
- [17] F. P. Heßberger, S. Hofmann, B. Streicher, B. Sulignano, S. Antalic, D. Ackermann, S. Heinz, B. Kindler, I. Kojouharov, P. Kuusiniemi, M. Leino, B. Lommel, R. Mann, A. G. Popeko, Š. Šáro, J. Uusitalo, A. V. Yeremin, *Eur. Phys. J.* **A41** (2009) 145–153.
- [18] F. P. Heßberger, S. Hofmann, D. Ackermann, V. Ninov, M. Leino, G. Münzenberg, Š. Šáro, A. Lavrentev, A. G. Popeko, A. V. Yeremin, Ch. Stodel, *Eur. Phys. J.* **A12** (2001) 57–67.
- [19] G. Audi, F. G. Kondev, Wang Meng, W. J. Huang, S. Naimi, *Chin. Phys.* **C41** (2017) 030001.